Journal of Environmental Management 395 (2025) 127782

Contents lists available at ScienceDirect

Journal of Environmental Management

journal homepage: www.elsevier.com/locate/jenvman

Research article

The role of agricultural fertilization intensity on fluvial GHG fluxes from tropical and temperate catchments

Ricky Mwangada Mwanake [a,*], Gretchen Maria Gettel [b,d], Elizabeth Gachibu Wangari [a], Klaus Butterbach-Bahl [a,c], Ralf Kiese [a]

[a] Karlsruhe Institute of Technology, Institute for Meteorology and Climate Research, Atmospheric Environmental Research (IMK-IFU), Kreuzeckbahnstrasse 19, Garmisch-Partenkirchen, 82467, Germany
[b] IHE-Delft Institute for Water Education, Westvest 7, 2611 AX, Delft, the Netherlands
[c] Pioneer Center Land-CRAFT, Department of Agroecology, University of Aarhus, Denmark
[d] Department of Ecoscience, Lake Ecology, University of Aarhus, Denmark

ARTICLE INFO

Keywords:
Carbon dioxide
Methane
Nitrous oxide
Source partitioning

ABSTRACT

Catchment land use intensity can influence C and N cycling within streams, with implications for fluvial greenhouse gas (GHG) fluxes (CO_2, CH_4, N_2O). This study analyzed annual datasets of hydrological, water physico-chemical parameters, GHGs saturations (%), and their fluxes from 78 stream sites in tropical and temperate catchments with contrasting agricultural fertilization intensities. In both climatic regions, instream GHG saturations correlated negatively with dissolved oxygen and mainly positively with dissolved inorganic nitrogen (DIN) ($p < 0.05$, $r^2 = 0.30–0.49$), suggesting nitrogen-driven biogenic GHG production. In contrast to these similarities, agricultural intensity shaped how fluvial GHG fluxes scaled with distal drivers such as stream size, land use, and discharge. In tropical catchments with mainly extensive agriculture, CO_2, and N_2O fluxes decreased with stream size ($p < 0.05$, $R^2 = 0.77–0.82$). However, in temperate catchments with intensive agriculture, land use was more important than stream size, with DIN concentrations and GHG fluxes increasing with agricultural land use ($p < 0.05$, $R^2 = 0.46–0.53$). Agricultural fertilization intensity also seemed to influence CO_2 sources during high-discharge events across the two study regions. Based on inferences from the respiratory quotient (range; 0.5–2.8), peak CO_2 fluxes in the tropical catchments were linked to external CO_2 inputs, while those in the temperate catchments linked to instream respiration under elevated nitrogen conditions. The findings of this study show that it is essential to consider gradients of agricultural fertilizer intensity to scale fluvial GHG emissions with their distal drivers, information critical for upscaling reach-scale GHG emissions.

1. Introduction

Prior to the 21st century, fluvial ecosystems were considered passive conduits for dissolved and particulate organic carbon and nitrogen moving from terrestrial environments to the oceans (Hynes, 1975). However, by the first decade of the 21st century, ecologists had demonstrated that these ecosystems are active pipes that process terrestrially derived carbon and nitrogen, releasing significant amounts of greenhouse gases (GHGs: CO_2, CH_4, and N_2O) into the atmosphere (Raymond et al., 2013; Rocher-Ros et al., 2023; Yao et al., 2020). It is estimated that these GHG emissions from fluvial ecosystems are substantial, contributing approximately 14 % (7.6, range; 6.1–9.1 Pg-CO_2-eq yr^{-1}) of the global anthropogenic CO_2-equivalent emissions (Jones et al., 2023; Li et al., 2021). Yet, despite the importance of fluvial ecosystems as net sources of GHGs, the critical factors controlling the magnitude of emissions are still marred with uncertainties due to the paucity of detailed field measurements in space and time that allow for such in-depth analysis (Lauerwald et al., 2023).

Several studies have demonstrated that GHG fluxes from streams are influenced by in-stream water quality parameters such as labile forms of organic matter (OM) and nitrogen (Borges et al., 2015; DelVecchia et al., 2023; Lauerwald et al., 2023; Mwanake et al., 2025a). For example, higher OM levels tend to support increased microbial respiration and methanogenesis, leading to higher CO_2 and CH_4 fluxes (e.g., Borges et al., 2015; Stanley et al., 2016), while also affecting N_2O fluxes depending on NO_3 availability (e.g., Mwanake et al., 2019; Mwanake

* Corresponding author.
E-mail address: ricky.mwanake2@kit.edu (R.M. Mwanake).

https://doi.org/10.1016/j.jenvman.2025.127782
Received 2 September 2025; Received in revised form 16 October 2025; Accepted 22 October 2025
Available online 26 October 2025

et al., 2025a). On the other hand, elevated nitrogen concentrations can further promote N_2O and CO_2 production through processes like nitrification, respiration, and denitrification (e.g., Andrews et al., 2021; Bodmer et al., 2016; DelVecchia et al., 2023).

Landscape characteristics such as stream size, slope, catchment topography, and land use have also been shown to influence GHG emissions either indirectly by affecting the input of OM and nitrogen to streams, or directly through the inputs of dissolved GHGs (e.g., Herreid et al., 2021; Mwanake et al., 2023a; Park et al., 2023; Rocher-Ros et al., 2023). For instance, smaller streams often exhibit higher GHG emissions due to increased surface connectivity with surrounding landscapes, which serve as external GHG sources and supply both OM and nitrogen for internal GHG production (Li et al., 2021). However, the extent of these inputs largely depends on the surrounding land use and its intensity, with some studies showing that streams draining intensive agricultural areas with significant fertilization rates receive more dissolved GHG and nitrogen inputs, resulting in higher fluvial GHG fluxes (Borges et al., 2018; Mwanake et al., 2023a; Upadhyay et al., 2023). Yet, due to the few comparative studies on stream size and land use effects on fluvial GHG concentrations or fluxes (e.g., Borges et al., 2018; DelVecchia et al., 2023; Mwanake et al., 2022), it remains unclear what environmental conditions one of them dominates when it comes to predicting their spatio-temporal variability. Such information is vital for scaling up fluvial GHG fluxes from reach scales to broader spatial scales, which has been previously shown to mainly depend on both stream size and catchment land use (Mwanake et al., 2022; Wallin et al., 2018).

Similar to catchment land use and stream size effects, seasonal variations in precipitation and temperature can cause variations in fluvial GHG concentrations and fluxes by affecting stream air-water gas exchange rates and the rates of biogeochemical reactions involved in GHG production and consumption (Aho et al., 2021, 2022; Mwanake et al., 2023a; Raymond et al., 2012). While intrannual temperature changes may play a more significant role in controlling instream biogeochemical GHG production within temperate climates, precipitation events can affect both the physical and biogeochemical drivers of fluvial GHG emissions irrespective of climatic region, thereby exerting greater control over their annual emissions. For example, heavy precipitation events result in high discharge periods, which can increase the supply of dissolved GHGs from external sources and offset the reduced contribution of internal GHG production due to shorter water residence times (e.g., Liu et al., 2023; Liu et al., 2022; Piatka et al., 2024). In contrast, periods of minimal precipitation, which are often characterized by lower stream discharge with significant groundwater inputs and longer water residence times, are hot moments for in-situ C and N cycling and associated GHG production (e.g., Borges et al., 2018; Mwanake et al., 2023b).

Based on changes in instream discharge, it may be possible to infer the dominance of internal or external sources of fluvial GHG emissions, which is information that may be key to informing future mitigation strategies, especially as extreme discharge events are projected to increase with climate change (Battin et al., 2023). Yet, studies of seasonal GHG variations in streams in the context of intra-annual discharge variability are still limited (Lauerwald et al., 2023), making it challenging to use discharge as a proxy to partition these two primary GHG sources in fluvial ecosystems and how land use and land use intensity may affect them.

The main objective of this study was to use year-long tropical and temperate field datasets developed with similar methodological approaches to compare the intra-annual drivers of fluvial GHG fluxes between two contrasting regions. The first was a European temperate region, characterized mainly by intensive agriculture, and the second was in the African tropics, characterized by mostly extensive agriculture. Unlike other studies that only examined land use and stream order effects on regional scales (e.g., Borges et al., 2018; DelVecchia et al., 2023), our study aimed to compare the dominance of these two factors across climatic zones that differed mainly in their agricultural fertilization intensities. Specifically, we aimed to determine 1.) the relative roles of stream discharge and biogeochemical parameters in controlling fluvial GHG saturation, 2.) the relative roles of stream size and catchment land use as drivers of the fluvial GHG fluxes along agricultural fertilization intensity gradients, and 3.) the potential of stream discharge as a proxy for partitioning internal vs. external sources of fluvial GHG fluxes.

We hypothesized that the drivers of fluvial GHG saturations and fluxes across the two study regions would be mainly similar, driven by similarities in the physical and biogeochemical processes that characterize headwater streams. However, the magnitude of the effects of both instream water quality parameters and landscape characteristics on fluvial GHG dynamics would depend on the fertilization intensity. Specifically, streams in intensively fertilized agricultural areas characterized by increased N inputs would contribute disproportionately high GHG emissions than those within extensive fertilized agricultural areas. We also hypothesized that the main sources of fluvial GHGs can be identified by combining changes in in-stream discharge conditions with quantitative measures of autochthonous GHG production processes versus allochthonous inputs, such as the respiratory quotient.

2. Materials and methods

2.1. Datasets

For this comparative study, we used previously published datasets from 78 stream sites that included water quality variables, GHG concentrations, and estimated GHG fluxes from 23 temperate sites in Germany and 55 tropical sites in Kenya (Table 1; Mwanake, 2023a, 2023b). The compiled dataset was unique as it was developed using similar quantitative methods and covered annual temporal trends of GHG emissions from different land uses/land covers (forests, croplands, urban regions, grasslands, and wetlands), stream sizes (Stream orders 1–6), and regions (tropical and temperate). In brief, the tropical sites were located in the Kenyan portion of the Mara River basin (~8400 km^2). Two main tributaries form the upper part of the basin, the Nyangores and Amala streams, with an additional tributary, Talek, joining the Mara River before it crosses the border in the Maasai Mara National Park, which is an important tourist destination in the region. The Mara region experiences bimodal rainfall, with the first season from March to June (long rains) and the second season from October to December (short rains). The other months are mostly dry with little or no rainfall (Mwanake et al., 2022). The temperate sites were located from southern to central Germany, covering a wide range of elevations, similar to the Kenyan sites. The southernmost sites were located in the mountainous region within the Loisach catchment, while the other sites were located in the Neckar and Schwingbach catchments with moderate to low elevations. Precipitation as rainfall within the catchments mainly occurs during the summer months, particularly June and July, and reduces in late summer and autumn months from August to October. Winter months are mostly drier, with rainfall mainly falling as snow (Mwanake et al., 2023a).

Upstream catchment areas and stream orders across the 78 sites were delineated in QGIS from digital elevation models (DEM: resolution 25–30m). The upstream land uses % (also used from here on to describe land covers) of all the delineated catchments were calculated from the Corine land cover and land use 2018 survey (https://land.copernicus.eu/pan-european/corine-land-cover/clc2018?tab=mapview) for the temperate sites and the Sentinel 2 prototype land cover and land use map for Africa (ESA CCI LAND COVER – S2 prototype Land Cover 20m map of Africa, 2016) for the tropical sites. The rationale for using region-specific land use products was that both datasets incorporated regionally tailored classification schemes and training data, which resulted in more accurate and thematically detailed representations of their diverse individual landscapes that also matched our field observations. For the land use estimations for each catchment, land-use polygons from both

Table 1
Summary table indicating the sampling duration, number of sites, number of observations, ranges and means (± standard errors) of stream hydrological, water physico-chemical variables, GHG concentrations, and fluxes in the tropical and temperate catchments. Letters beside the mean indicate significant differences (p-value < 0.05) from Tukey post-hoc tests based on the analysis of variance from linear mixed effects models (Table A1).

	Tropical catchments (Nyangores, Amala, Talek)					Temperate catchments (Loisach, Neckar, Schwingbach)				
	Sampling period	Number of sites	Number of observations	Range	Mean ± SE	Sampling period	Number of sites	Number of observations	Range	Mean ± SE
Temperature (° C)	Annual	55	558	11.1–34.1	18.01 ± 0.13 **b**	Annual	23	413	0.9–23.8	10.2 ± 0.2 **a**
pH	Annual	55	452	6.04–9.2	7.36 ± 0.02 **a**	Annual	23	399	7.11–9.02	7.98 ± 0.02 **b**
DO saturation (%)	Annual	55	556	9.9–126.1	89.89 ± 0.65 **a**	Annual	23	399	54.6–143	94.15 ± 0.71 **a**
NH_4-N (mg L^{-1})	Annual	55	549	0.11–1.12	0.41 ± 0.01 **b**	Annual	23	366	0–0.45	0.09 ± 0.01 **a**
NO_3-N (mg L^{-1})	Annual	55	556	0.18–18.21	2.56 ± 0.11 **a**	Annual	23	400	0.02–18.1	3.08 ± 0.16 **a**
DOC (mg L^{-1})	Annual	55	543	0.8–25.04	4.69 ± 0.16 **b**	Annual	23	401	0.73–16.05	3.76 ± 0.09 **a**
DOC: NO_3 ratio	Annual	55	537	0.08–120.27	6.36 ± 0.48 **a**	Annual	23	392	0.23–169.17	4.41 ± 0.5 **a**
Discharge (L s^{-1})	Annual	55	516	0.01–47562.58	1766.46 ± 230.7 **a**	Annual	23	412	0.01–18523	370.45 ± 70.15 **a**
CO_2 saturation (%)	Annual	55	551	46–1933	392 ± 11 **a**	Annual	23	407	100–2003	534 ± 18 **a**
CH_4 saturation (%)	Annual	55	550	155–1631329	34,749 ± 4158 **b**	Annual	23	404	76–131,078	5937 ± 653 **a**
N_2O saturation (%)	Annual	55	551	36–1481	160 ± 6 **a**	Annual	23	402	8–5655	388 ± 32 **b**
CO_2-C flux (mg m^{-2} d^{-1})	Annual	55	530	−1238.42 - 64,878.06	4291.88 ± 293.88 **a**	Annual	23	406	−54.89 - 212,439.58	19,533.7 ± 1510.7 **b**
CH_4-C flux (mg m^{-2} d^{-1})	Annual	55	529	0.13–505.31	35.36 ± 2.39 **b**	Annual	23	403	−0.45 - 356.76	28.21 ± 2.5 **a**
N_2O-N flux (mg m^{-2} d^{-1})	Annual	55	529	−2.08 - 33.95	1.45 ± 0.17 **a**	Annual	23	401	−10.55 - 204.54	14.19 ± 1.54 **b**

datasets were clipped to match the catchment boundaries delineated for each site using the digital elevation model (DEM). The area of each land-use class within a catchment was then calculated and expressed as a percentage of the total catchment area. Finally, all land-use classes associated with agricultural activities (e.g., croplands and fertilized grasslands) within each site were aggregated into a single category representing total agricultural land use. Generally, the percentage of agricultural land use ranged from 0 to 100 across both regions. The number of sampled lower-order streams (stream order 1–3) was higher than that of higher-order streams in both study regions, following the natural order of their abundance in distribution (Table S1).

Sampling across the 78 sites was done on a triweekly-monthly basis between January 2019 and February 2020 in the Amala, Nyangores, and Talek catchments, between June 2020 and June 2021 in the Loisach and Schwingbach catchments, and between April 2021 and April 2022 in the Neckar catchment. For each site visit, discharge at most streams was calculated using the velocity area method based on stream width, depth, and velocity (OTT-MF-Pro, Hydromet, Germany) measurements. For large rivers that were not wadable (stream order 6) during high discharge, velocity was measured using floating oranges, depth was obtained directly from gauging stations, while discharge was either calculated using the velocity area method or obtained from water authorities. The stream slope at each sampling point over a ~5m reach was also measured using a laser rangefinder with a slope function (Nikon Model: 8381, Japan).

Water temperature (°C), pH, and dissolved oxygen (DO) (% saturation) were quantified in situ using the Pro DSS multiprobe (YSI Inc., USA). Water samples for ammonium, nitrate, and dissolved organic carbon (DOC) analyses were collected and filtered on-site (polyethersulfone (PES) and glass fiber filters, pre-leached with 60 ml of miliq water). In the laboratory, these samples were analyzed for NH_4-N and NO_3-N concentrations using colorimetric methods by measuring the absorbance of the samples using a microplate spectrophotometer (Model: Epoch, BioTek Inc., USA). The DOC concentrations were measured as non-purgeable organic carbon (NPOC) using a TOC/TN analyzer (Analytica-Jena; multi N/C 3100, Germany and Shimadzu TOC-L, Japan).

CO_2, CH_4, and N_2O concentrations in the streams were sampled in situ using the headspace equilibration technique and analyzed on a GC (8610C, Germany). Stream water CO_2, CH_4, and N_2O concentrations (mass m^{-3}) were then calculated based on their Henry's solubility constants. All the gas concentrations were then expressed as percent saturations relative to their equilibrium concentrations to correct for temperature effects on gas solubilities and allow for inter-climatic comparisons.

Daily diffusive fluxes (F) (mass m^{-2} d^{-1}) of the three GHGs were estimated using Fick's Law of gas diffusion, where the flux is the product of the gas exchange velocity (k) (m d^{-1}) and the difference between the stream water (C_{aq}) and the ambient atmospheric gas concentration in water assuming equilibrium with the atmosphere (C_{sat}) (Equation (1)). The temperature-specific gas transfer velocities (k) for each of the gases were calculated from an ensemble mean of three normalized gas transfer velocities (k_{600}) (m d^{-1}) modeled from measured stream velocity (m s^{-1}) and the slope (m m^{-1}) values using equations (3)–(5) from Raymond et al. (2012) (Fig. S1). The rationale for using these three equations is that they apply across a wide range of river sizes and align with the general theoretical expectation that, as stream order increases, watershed slope decreases and velocity increases predictably (Raymond et al., 2012). A detailed description of the study areas, analytical methods, and seasonal effects (dry and wet in the tropics and summer, autumn, winter, and spring in the temperate region) on the riverine GHG fluxes can be found in the respective individual publications (Mwanake et al., 2022, 2023a).

$$F = k\left(C_{aq} - C_{sat}\right) \quad (1)$$

2.2. Statistical analysis

A one-way analysis of variance followed by a Tukey post-hoc test using linear mixed-effects models was conducted to identify significant differences ($p < 0.05$) in discharge, water-physicochemical variables, and GHG fluxes between the tropical and temperate catchments. To ensure that the assumption of normality was met for this analysis, several parameters with skewed distributions (discharge, NH_4, DOC: NO_3 ratio, and GHG saturation and fluxes) were transformed using the natural logarithm. The advantage of using mixed effects models is that they allow for the determination of the variance explained by both fixed and random effects, and they are less sensitive to unequal class observations. Consequently, the overall model performance (indicated by the conditional r^2 and the distribution of the residuals (normally distributed with a mean close to zero: Fig. S2)) was assessed based on the variance explained by both fixed effects (tropical vs temperate; indicated by the marginal r^2) and random effects (site and sampling date).

Elastic net regression models were used in tropical and temperate catchments to determine the relative roles of discharge and biogeochemical variables in controlling riverine GHG concentrations. The advantage of using these models was that they performed lasso regressions, which automatically removed nonsignificant independent variables by assigning them a coefficient of zero, and also ridge regressions, which reduced the impact of the multicollinearity of the independent variables by shrinking of coefficients (Zou and Hastie, 2005). In addition, the standardized slope coefficients provided by these models enabled the determination of the most important predictor variables. The independent variables in the elastic net regression models included discharge and water-physicochemical variables (DO saturation, NO_3, NH_4, DOC, and DOC: NO_3 ratio) that have previously been shown to influence the magnitude of fluvial GHG production processes (Battin et al., 2023; Mwanake et al., 2025a; Quick et al., 2019; Stanley et al., 2016; Taylor and Townsend, 2010). To meet the normality assumption of the dependent variable for this analysis, we used the transformed GHG saturation data (natural logarithm).

Simple bivariate regression analyses were used to compare the role of catchment land use and stream size as drivers of water quality and fluvial GHG fluxes between the two study regions. Independent variables in these analyses were stream order (represents stream size) and the upstream land use percent. In addition to analyzing the effects of stream order and catchment land use on instream water quality and GHG fluxes, we also looked into the role of agricultural land use intensity, which mainly varied between the tropical and temperate regions. To achieve this, we calculated an agricultural fertilization intensity index that included both the site-level percentage of agricultural land (cropland + pasture) and regional fertilizer input features. First, the site-level agricultural land use percentage was rescaled between 0 and 1 to make comparisons easier across locations. Simultaneously, we built a regional fertilization intensity index using five average indicators from Kenya, where the tropical sites are located, and Germany, where the temperate sites are situated. These country-level fertilization intensity indicators included the average synthetic fertilizer use for 2022 in kg ha^{-1} yr^{-1}(NPK: 35.06 for Kenya, 116.7 for Germany), excess nitrogen input in tonnes (111,723 for Kenya vs. 807,424 for Germany), excess phosphorus input in tonnes (55,254 for Kenya vs. 58,212 for Germany), total nitrogen input in tonnes (164,353 for Kenya vs. 1840000 for Germany), and total phosphorus input in tonnes (68,487 for Kenya vs. 294,231 for Germany) (Data source: https://ourworldindata.org/). Each variable was normalized to a zero value (lowest) or 1 (highest) value across the two regions, and the fertilization intensity index was calculated as the mean of the scaled values for each area. Finally, the agricultural fertilization intensity index was computed as the average of the scaled agricultural land use percent and the fertilization intensity index, giving equal weight (50 %) to local land use and regional fertilization rates and their pollution consequences. We then used a simple bivariate regression analysis to investigate the effects of agricultural fertilization intensity on key water quality parameters and fluvial GHG fluxes across the two study regions.

To determine how discharge regulates the contribution of internal GHG production vs. external sources, stream discharge was first classified into three main categories (low, medium, and high). Briefly, each sampling date for each stream was classified according to whether the normalized discharge (calculated by dividing each absolute discharge for each site visit during the year by the maximum measured discharge) fell within the 0–33 % percentile (low), 34–66 % (medium), or 67–100 % (high) days (e.g., Mwanake et al., 2022). For each of the three discharge categories, the stream respiratory quotient, which is estimated as the ratio of excess CO_2 (CO_2 dissolved in water – CO_2 in equilibrium with the atmosphere) to apparent oxygen utilization during respiration (AOU: O_2 dissolved in water – O_2 in equilibrium with the atmosphere), was calculated to determine the dominance of in-situ production over external sources (Richey et al., 1988). CO_2 was used for the analysis because of its dominance over N_2O and CH_4 in accounting for the total annual fluxes and the ease of interpreting its relationship with O_2. A respiratory quotient of <1.2 indicates the strength of aerobic respiration in accounting for in-situ CO_2 production, while an RQ > 1.2 indicates allochthonous inputs of dissolved CO_2 or anaerobic respiration (Richey et al., 1988).

3. Results

3.1. General comparisons between the tropical and temperate catchments

Discharge within the two study regions ranged over seven orders of magnitude, with the mean annual discharge being one order of magnitude higher in the tropical catchments than in the temperate catchments, although this difference was not significant (p-value >0.05) (Table 1, Table A1). In contrast to discharge, water temperature and pH differed significantly between the two study regions, with higher temperatures in the tropical catchments and higher pH in the temperate catchments (Table 1, Table A1). DO saturation varied by up to 2 orders of magnitude, with higher variability found in the tropical catchments than in the temperate catchments. No difference in DO saturation was found between the two study regions (Table 1, Table A1).

In the two study regions, NH_4-N, NO_3-N, and DOC concentrations varied by up to three orders of magnitude, with the latter two showing the highest spatio-temporal variability. NH_4-N and DOC concentrations were 1–4.5 times higher in the tropical catchments than in the temperate ones (Table 1, Table A1). Contrastingly, NO_3-N concentrations showed no significant differences between the two study regions but tended to be higher in the temperate catchments. DOC:NO_3 ratios were highly variable, ranging up to 5 orders of magnitude, with the lowest mean value recorded for the temperate catchments as compared to the tropical catchments, although the difference was insignificant (Table 1, Table A1).

GHG saturations were also highly variable in space and time, with the highest variability of up to 4 orders of magnitude recorded for CH_4 values. Comparing the two study regions, CO_2 saturation was 1.4 times higher in the temperate catchments than in the tropical catchments, but this difference was insignificant (p-value<0.05: Table 1). At the same time, opposite trends were found for CH_4 saturation, which was 5.8 times higher in the tropical catchments. N_2O saturation was twice as high in the temperate catchments than in the tropical catchments.

Like the GHG saturations, the fluxes were also highly variable in space and time, with predominantly positive flux values in both study regions, indicating that the streams were significant sources of GHGs to the atmosphere (Table 1). CO_2 and N_2O fluxes were 4–10 times higher in the temperate catchments than in the tropical catchments, while CH_4 fluxes showed opposite trends and were higher in the tropical catchments than in the temperate catchments (Table 1).

3.2. Effects of hydrology and water quality on fluvial GHG % saturations

The elastic regression models showed that both discharge and biogeochemical parameters were significantly ($p < 0.05$) related to GHG saturations, with r^2 values ranging from 0.30 to 0.49 (Fig. 1). The GHG % saturations across the two study regions mostly showed similar relationships with these parameters, albeit with different magnitudes. Judging by the magnitude of the standardized slope estimates, DO saturation and discharge had the most substantial relationship with CO_2 saturation in tropical catchments, while in temperate catchments, DO saturation and NO_3-N concentrations were the strongest predictors. Moreover, CO_2 saturation in the temperate catchments was positively related to water temperature, NH_4-N, and NO_3-N concentrations and negatively related to discharge, DO saturation, and DOC concentration (Fig. 1). Similar relationships were also found in the tropical catchments, except for water temperature and NH_4-N, which were insignificant.

Like CO_2 saturation, DO saturation was the strongest predictor of CH_4 saturation, with NO_3-N and water temperature being the other important parameters in tropical and temperate catchments. CH_4 saturation was positively related to NH_4-N concentration, water temperature, and the DOC:NO_3 ratio and negatively related to discharge and DO saturation (Fig. 1). However, opposite trends were found for NO_3-N concentration, which was positively related to CH_4 saturation in the temperate catchments and negatively related in the tropical catchments.

Similar to CO_2 and CH_4, DO saturation strongly predicted N_2O saturation across both catchments, with NO_3-N and water temperature being the other two important predictors of N_2O (Fig. 1). N_2O saturation was positively related to water temperature, NH_4-N, and NO_3-N concentrations in both study regions and negatively related to discharge and DO concentrations (Fig. 1).

3.3. Effects of stream size, agricultural land use, and fertilization intensity on fluvial GHG fluxes

Increases in stream discharge were related to increasing stream orders in the temperate and tropical catchments but had no significant relationship with catchment agricultural areas and the agricultural fertilization intensity (Fig. 2). Dissolved inorganic nitrogen (NH_4-N + NO_3-N) concentration increased with stream order in temperate catchments but decreased in tropical ones (Fig. 2). DIN concentrations also increased with larger agricultural areas in both regions, and were positively correlated with the agricultural fertilization intensity, showing higher DIN at more intensively fertilized agricultural sites in the temperate region (Fig. 2). DO saturation was positively related to stream order in both catchments, albeit the relationship was only significant in the temperate catchments (Fig. 2). Stream order had no significant relationship with the DOC:NO_3 ratio. However, decreases in the

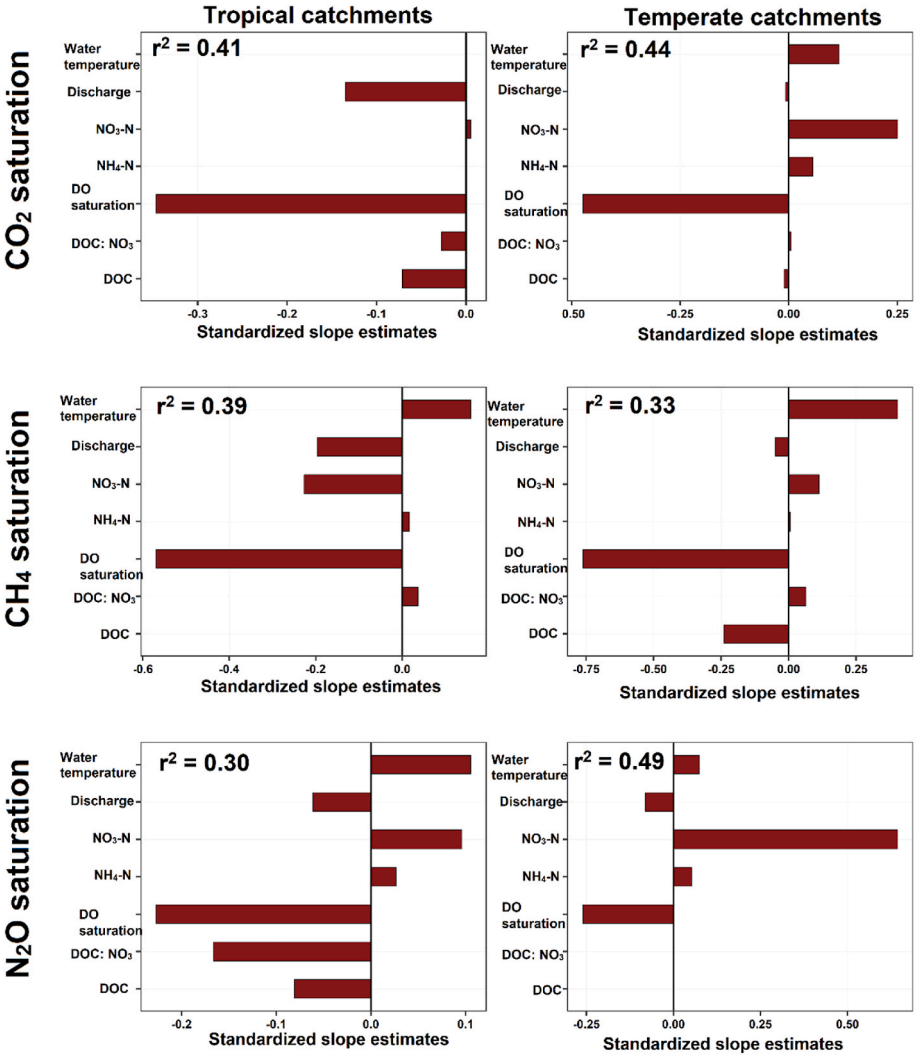

Fig. 1. Standardized slope plots of significant elastic net models predicting CO_2, CH_4, and N_2O concentrations (% saturations) from discharge, water temperature, DO % saturation, NH_4-N, NO_3-N, DOC, DOC: NO_3 ratio at the tropical and temperate catchments. Text on the graphs indicates the overall r^2 of the models.

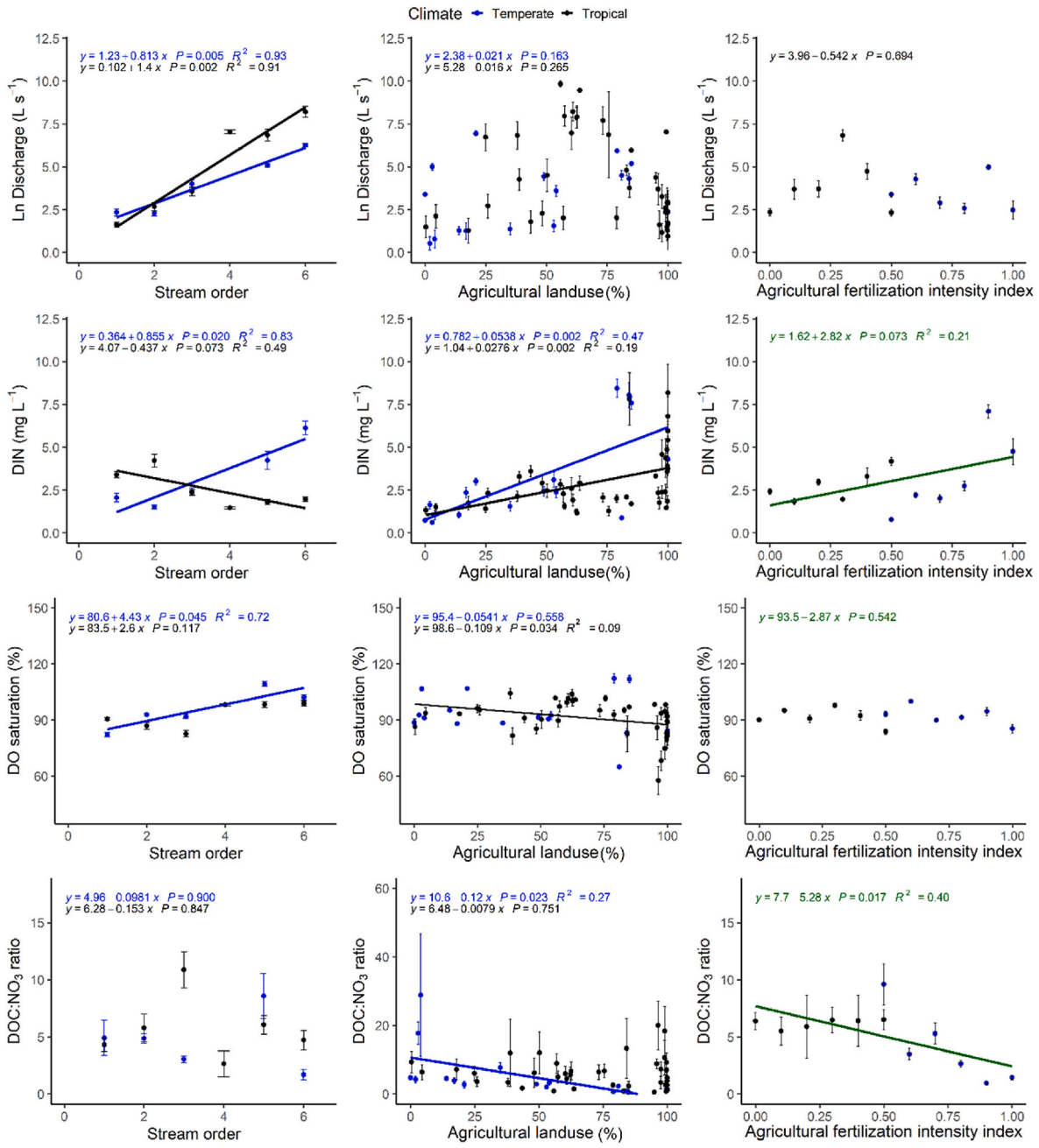

Fig. 2. Scatter plots of mean annual discharge and selected water quality variables against stream order, agricultural area and the agricultural fertilization intensity index in tropical catchments (in black) and temperate catchments (in blue). Points and error bars represent means ± SE of the respective parameters across the entire duration of sampling, and equations on the graphs indicate significant ($p < 0.05$) or marginally significant ($p < 0.1$) linear relationships.

DOC:NO_3 ratio were related to increasing agricultural areas in the temperate catchments, and also the overall increasing agricultural fertilization intensity from the tropical to the temperate catchments (Fig. 2).

In terms of GHG fluxes, CO_2 fluxes were negatively related to stream order in the tropical catchments, but there was no similar relationship in the temperate catchments. In contrast, CO_2 fluxes were positively related to agricultural areas in both catchments, with the slope of the relationship being 2 times higher in temperate catchments than tropical ones (Fig. 3). CH_4 fluxes had no significant relationships with stream order in either study area. However, increases in CH_4 fluxes were related to increasing agricultural areas, but only in the temperate catchments (Fig. 3). Like DIN, N_2O fluxes were positively related to stream order in the temperate catchments and negatively related to stream order in the tropical catchments (Fig. 3). An increase in agricultural area was related to increases in N_2O fluxes in both catchments, similar to what was found for CO_2 fluxes, but the slope of this relationship was 6.7 times higher in temperate catchments than tropical ones (Fig. 3). The stronger positive slopes linking agricultural areas to CO_2 and N_2O fluxes in the two climatic regions were explained by differences in agricultural fertilization intensity, which was significantly positively related to both fluxes across regions (Fig. 3).

3.4. *Effect of seasonality in discharge on fluvial GHG fluxes*

Total daily CO_2-equivalent fluxes, which include contributions from CO_2, CH_4, and N_2O fluxes, showed similar increasing responses to increased discharge in both study regions but with slightly different

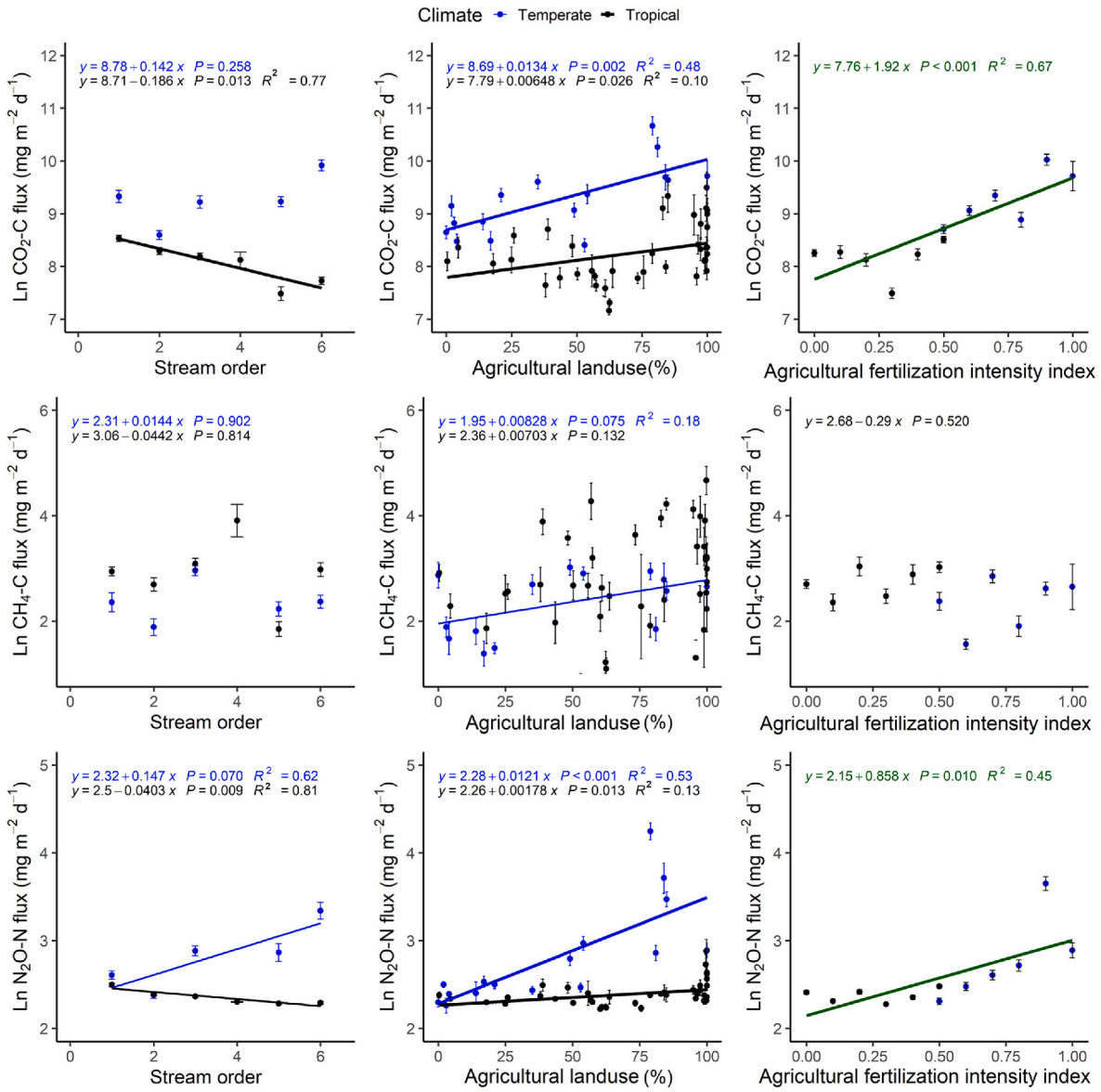

Fig. 3. Scatter plots of mean annual GHG fluxes against stream order, agricultural (cropland + pasture) area, and the agricultural fertilization intensity index in tropical catchments (in black) and temperate catchments (in blue). Points and error bars represent site-scale means ± SE of the respective parameters across the entire duration of sampling, and equations on the graphs indicate significant ($p < 0.05$) or marginally substantial ($p < 0.1$) linear relationships.

patterns (Fig. 4). The temperate catchments had overall higher CO_2-eq emissions than the tropical catchments, mainly due to higher CO_2 and N_2O fluxes, which contributed >97 % of the total emissions (Fig. 4). While the response to increasing discharge conditions in the tropical catchments was mainly linear, with CO_2-eq emissions almost doubling for each increment in discharge from low > medium > high, the increase in the emissions in the temperate catchments appeared to peak in the medium discharge period, before declining slightly in the high discharge period (Fig. 4).

3.5. *Effect of stream discharge on the respiratory quotient*

Significant positive relationships were found between excess CO_2 and AOU for all discharge conditions in the tropical and temperate catchments. However, the magnitude of the slope representing the respiratory quotient varied with region and discharge conditions (Fig. 5). In the temperate catchments, the respiratory quotient ranged from 0.54 to 0.61 and was primarily similar across the three discharge conditions, with only a slight decrease from low to high discharge conditions (Fig. 5). In contrast to the temperate catchments, the respiratory quotient was more variable across discharge conditions in the tropical catchments, ranging from 0.69 to 2.78, representing a 400 % increase in the respiratory quotient from low to high discharge conditions (Fig. 5).

4. Discussion

In this study, the in-depth analysis of critical direct and indirect drivers of intra-annual fluvial GHG dynamics complements previous similar efforts (DelVecchia et al., 2023; Marx et al., 2017; Quick et al., 2019; Stanley et al., 2016) by investigating how the dominance of the individual drivers on fluvial GHG fluxes changes depending on agricultural fertilization intensity (Fig. 2; Fig. 3). This analysis was made possible by using a unique GHG dataset previously collected with similar methodological approaches in two contrasting study regions, comprising tropical catchments in Kenya dominated by low agricultural fertilization intensity and temperate catchments in Germany with high agricultural fertilization intensity (Mwanake et al., 2022; Mwanake et al., 2023a; Václavík et al., 2013). In agreement with our hypothesis,

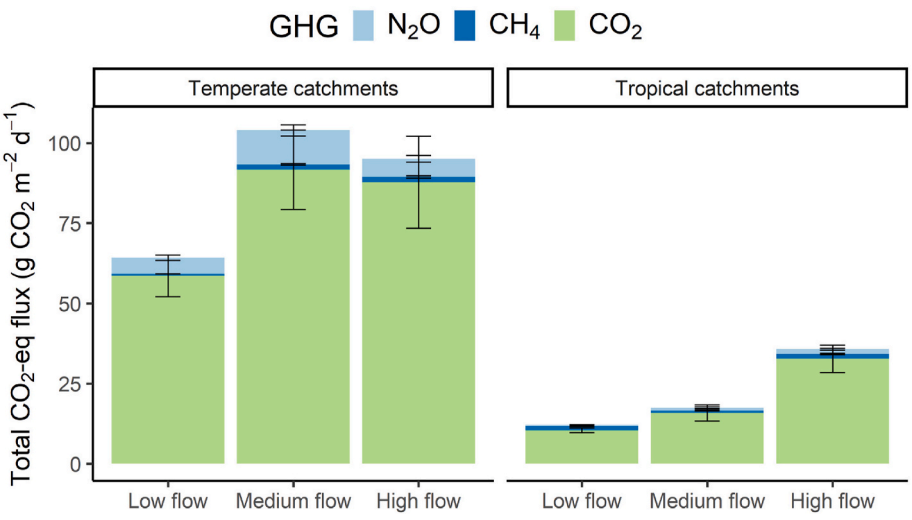

Fig. 4. Riverine CO_2-equivalent fluxes (mean ± SE) grouped by GHG type for each discharge category in the temperate and tropical catchments.

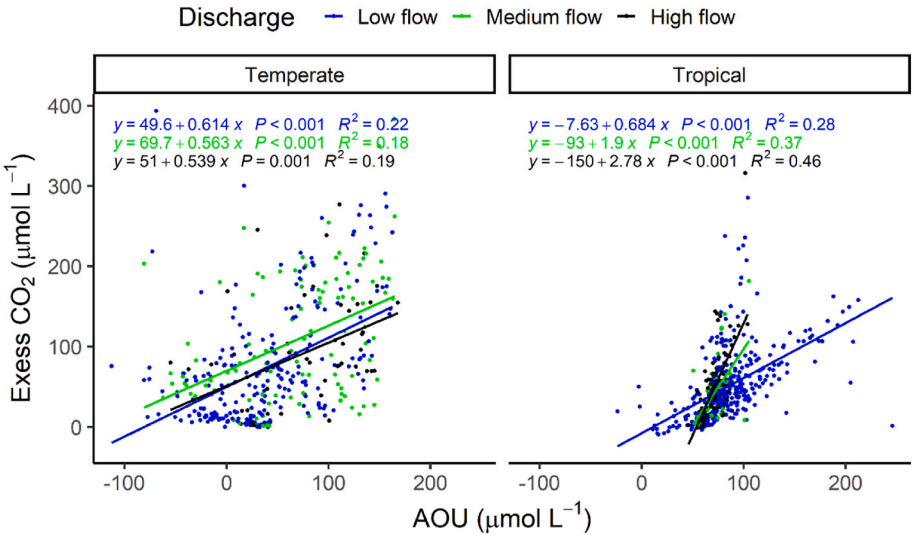

Fig. 5. Scatter plot of excess CO_2 (difference from equilibrium) produced against the apparent oxygen utilization (AOU) during respiration for the tropical and temperate catchments during the low, medium, and high discharge periods. Lines and equations on the graphs indicate significant ($p < 0.05$) linear relationships, with the slope value representing the respiratory quotient.

the role of instream water quality parameters, such as water temperature, inorganic nitrogen, and organic carbon, was identical in the two study regions, potentially reflecting the similarity in the underlying biogeochemical processes (Fig. 1). However, the role of drivers, such as stream size, catchment land use, and discharge, which are mainly used in the spatial upscaling of fluvial GHG fluxes (e.g., Mwanake et al., 2022; Wallin et al., 2018), differed depending on catchment-specific conditions linked to the agricultural fertilization intensity (Figs. 2–5).

4.1. *Agricultural fertilization intensity effects on fluvial GHG fluxes*

Catchment land use resulted in differences in fluvial GHG emissions, similar to previous studies conducted along land use gradients (e.g., Herreid et al., 2021; Ho et al., 2022; Stanley et al., 2016). However, the magnitude of the effects of land use seemed to depend further on the intensity of agricultural fertilization (e.g., Mwanake et al., 2025b), which differed across the two study regions. For example, CO_2 and N_2O fluxes were up to 10 times higher in the temperate catchments than in the tropical catchments, suggesting that enhanced instream nutrient levels resulting from higher agricultural fertilization rates in the temperate catchments likely favored CO_2 and N_2O production from respiration, nitrification, and denitrification (e.g., Bodmer et al., 2016; Mwanake et al., 2024; Wang et al., 2024). This conclusion also agrees with the increase in in-stream DIN concentrations and decrease in DOC:NO_3 ratios with increasing agricultural fertilization intensity across the two climatic regions (Fig. 2), indicating elevated nitrogen inputs in the temperate streams due to intensive fertilizer application (e.g., Wachholz et al., 2023). We also found direct positive relationships between CO_2 and N_2O saturation with inorganic nitrogen (Fig. 1), further indicating the importance of elevated nitrogen in increasing fluvial GHG % saturation. DelVecchia et al. (2023), in their study of 27 streams and rivers across multiple ecoclimatic regions of the United States, found that all three GHG variabilities could be explained by in-stream TN concentrations, suggesting a similar control that increased N availability positively influenced CO_2 and N_2O production processes. In contrast to CO_2 and N_2O, DOC:NO_3 ratios and CH_4 fluxes were higher in the tropical catchments with less agricultural fertilization intensification than in the temperate catchments, indicating much more favorable environmental conditions in these catchments that supported elevated CH_4 production through methanogenesis (Table 1). This conclusion is also consistent

with the negative relationship of CH_4 with electron acceptors such as DO and NO_3 in the tropics (Fig. 1), which are conditions previously associated with highly reduced redox conditions that drive in-stream methanogenesis (Baulch et al., 2011; Qin et al., 2020; Schade et al., 2016). Despite similar negative relationships with DO in the tropical sites, N_2O and CH_4 showed contrasting associations with NO_3, indicating that their production pathways operate under distinct redox regimes (Helton et al., 2015). The strongly reducing conditions, marked by both low DO and NO_3 concentrations in tropical sites, may have favored both methanogenesis and N_2O reduction to N_2, ultimately resulting in lower N_2O fluxes compared to the temperate sites.

4.2. Stream size vs. catchment land use along agricultural fertilization intensity gradients

Although instream nitrogen and riverine GHG fluxes are known to naturally decrease with stream size/order due to disproportionately higher benthic, groundwater, and terrestrial contributions in small streams compared to large streams (e.g., Hotchkiss et al., 2015; Marzadri et al., 2017), we found contrasting trends between the two study regions that differed in agricultural fertilization intensity (Figs. 2 and 3). In the tropical catchments, which were mainly dominated by extensive pastures and croplands with generally low N fertilizer application, DIN concentrations, CO_2, and N_2O fluxes decreased significantly with stream order, following the expected natural trends linked to the levels of stream-terrestrial-groundwater connections. In contrast to the tropical catchments, DIN concentrations, CO_2, and N_2O fluxes tended to increase with increases in stream order in the temperate catchments with intensive agricultural areas, indicating a potential breakdown of the expected stream order nutrient and GHG relationships in catchments dominated by intensive agricultural areas with higher fertilization rates (e.g., Borges et al., 2018; DelVecchia et al., 2023; Marescaux et al., 2018). These results suggest that yearlong point (tile drainage pipes) or diffuse (surface and sub-surface) nutrient and labile carbon supply to large streams, which create ideal conditions for GHG production processes such as respiration for CO_2 and nitrification-denitrification for N_2O, may outweigh the geomorphological disadvantages of larger streams (e.g., lower surface area to volume ratio for external GHG supplies) compared to much smaller streams. This conclusion is supported by the increases in instream DIN concentrations, CO_2 and N_2O fluxes with increases in agricultural fertilization intensities across the two climatic regions (Figs. 2 and 3).

The breakdown of stream order nutrient and GHG relationships in the temperate catchments of this study are also consistent with what was reported for multiple streams in the United States, which found that stream order was positively correlated with total nitrogen and showed no relationship with CO_2 and N_2O (DelVecchia et al., 2023). We argue that increases in agricultural fertilization intensity downstream of river networks may have accounted for these findings, considering that most of the USA, similar to the temperate catchments in this study, is mainly dominated by intensive agriculture in comparison to our tropical catchments (See Václavík et al., 2013).

In addition to agricultural intensification linked to fertilizer application rates, alterations to flow paths within river networks may also help explain the contrasting fluvial GHG fluxes and nutrient dynamics observed between our two study regions (e.g., Battin et al., 2023). For instance, a study of nutrient transport within the temperate U.S. Great Lakes basins found that overland flow and tile drainage systems accounted for the majority of total nitrogen (66 %) and phosphorus inputs (76 %) to streams (Wan et al., 2023). These engineered drainage networks, which are less common in tropical African regions like those in our study but more frequently found in our studied temperate catchments, may have reduced the travel time and distance for dissolved nutrients and dissolved GHGs through soils, ultimately increasing their loads to the streams.

4.3. Discharge as a proxy for internal vs. external GHG sources

In general, temperate catchments had more than double the total fluvial CO_2 equivalent emissions from tropical catchments, irrespective of discharge conditions (Fig. 4). These findings suggest that due to the higher agricultural intensification in these catchments (Figs. 2 and 3), elevated instream production of GHGs is favored by a steady supply of nutrients and labile carbon throughout the year. However, total daily CO_2 equivalent emissions in both study regions were 1–2 times higher in the medium and high discharge periods than in the low discharge period, indicating a positive effect of discharge on air-water gas exchange rates and external GHG sources, agreeing with findings from multiple other studies (e.g., Duvert et al., 2020; Liu et al., 2023; Piatka et al., 2024; Raymond et al., 2012). These positive trends were primarily associated with CO_2 fluxes, which accounted for more than 90 % of daily mean annual emissions, while N_2O and CH_4 were minor contributors (Fig. 4).

The positive response of GHG fluxes to discharge conditions in both study regions also suggested a lack of source limitation, likely due to either maintained levels of internal GHG production or sufficient external GHG sources combined with higher gas exchange rates. However, the effects of discharge on GHG fluxes appeared to further depend on the intensity of agricultural fertilization. In the temperate catchments with intensively managed agricultural areas, increased discharge had a less diluting effect on in-stream GHG saturation than in the extensively managed tropical catchments (Fig. 1), suggesting a lack of GHG source limitation during periods of increasing discharge in these catchments. A similar "chemostatic" response of in-stream GHG concentrations to discharge has also been found in previous temperate studies, suggesting similar controls of more steady supplies of GHGs that balance out the high evasion rates (Aho et al., 2021; Zannella et al., 2023). That said, we found that under increasing discharge conditions, fluvial GHG fluxes in the temperate sites plateaued at high discharge, while in the tropical sites, the fluxes increased linearly across the three discharge categories (Fig. 4). Although it is difficult to pinpoint the exact drivers of these contrasting regional patterns, we hypothesize that they may be due to differences in the relative influence of gas exchange rates versus in-stream GHG concentrations on overall GHG fluxes. In the temperate sites, high GHG fluxes may have been primarily driven by elevated in-stream GHG concentrations, which likely responded non-linearly to discharge due to the balance between evasion and replenishment by their sources. In contrast, in the tropical sites, higher gas transfer velocities, which typically increase linearly with discharge (See Raymond et al., 2012), may have played a more dominant role.

To infer the primary sources of fluvial GHGs under elevated discharge conditions in the two study regions, we hypothesized that changes in the respiratory quotient (RQ) during these periods could indicate the relative dominance of internal production processes versus external inputs of CO_2, which was also the most dominant GHG (Fig. 5). During low discharge, our results showed similar RQ values of ~0.7 in both study regions, which may indicate that aerobic respiration largely accounted for CO_2 fluxes during this period due to longer water residence times (e.g., Borges et al., 2018; Mwanake et al., 2023b). However, differences emerged between the two study regions with increasing discharge conditions. In temperate catchments dominated by intensively fertilized agricultural areas, increased discharge conditions had minimal effects on the RQ, which remained within the range of the 0.7 value. This finding may indicate that internal CO_2 production from respiration dominates in maintaining peak fluxes even under increased discharge conditions. Mechanistically, higher fertilization rates in temperate agricultural sites may have led to improved instream nutrient conditions, which have been shown to enhance elevated CO_2 production from microbial-mediated respiration (e.g., Dang et al., 2021; Kominoski et al., 2018). This conclusion is further supported by the lower DOC:NO_3 ratios observed at the temperate sites compared to the tropical sites (Table 1), which may reflect concurrent DOC losses due to enhanced respiration

under elevated NO_3 inputs in these ecosystems due to fertilization. In contrast to the temperate catchments, the RQ values in tropical catchments, mainly dominated by extensively managed agricultural areas with low fertilization rates, doubled at elevated discharge conditions. Such elevated RQ values > 1.2 during the wetter periods of the year suggest that inputs of dissolved CO_2 from the surrounding landscapes or enhanced instream weathering processes (e.g., Richey et al., 1988), may have maintained the elevated fluxes in the tropical catchments due to internal substrate limitation. While RQ values > 1.2 in the high discharge period may also imply anaerobic production of CO_2, this process is improbable to occur due to shorter water residence times and higher oxygen reaeration rates during the high discharge events.

4.4. Limitations of our approaches

While our study provides valuable insights into fluvial GHG sources across diverse streams differing in land use, climate, and topography, several sources of uncertainty should be acknowledged to better interpret our findings. First, the fluvial GHG fluxes reported here were estimated based on measured concentration gradients and modeled gas transfer velocities derived from stream geomorphological parameters. Although this approach is commonly applied, especially in small, turbulent headwater streams or in large-scale studies where direct methods such as floating chambers are impractical (Aho et al., 2021, 2022; Borges et al., 2015; Piatka et al., 2024), model-derived gas transfer velocities can introduce substantial uncertainty in flux magnitudes, which may range from low to high depending on individual sites (Hall and Ulseth, 2020; Raymond et al., 2012). Future studies should aim to directly measure gas transfer velocities in the field using tracer gases to reduce these uncertainties (Hall and Ulseth, 2020).

Second, our comparisons were based on datasets collected over multiple years of sampling. This temporal variability may introduce bias if significant interannual differences occurred, such as severe droughts or flooding events, which are known seasonal drivers of fluvial GHG emissions (Borges et al., 2018; Woodrow et al., 2024). However, we believe this effect was minimal, as land use and stream size, the primary broader-scale drivers of site-scale variation in fluvial annual GHG fluxes in both the tropics and temperate regions, remained relatively constant throughout the study period.

Third, the agricultural fertilization index used in this study was derived from national-scale fertilization statistics, which may not fully capture farm-specific differences in fertilizer amounts, type, and application frequency. These local variations are crucial for understanding spatial heterogeneity in riverine GHG fluxes, as they influence the timing and magnitude of fertilizer-derived nutrient inputs entering rivers. Future efforts to develop similar indices should therefore focus on acquiring finer-scale fertilization data through close collaboration with local stakeholders, such as farmers, particularly in regions characterized by fragmented agricultural ownership and limited centralized record-keeping.

Lastly, although the RQ value provided a valuable proxy for differentiating dominant fluvial CO_2 sources, threshold-based interpretations of this value (e.g., in this study and Richey et al., 1988) remain simplifications, as aerobic and anaerobic processes often co-occur within streams, and processes other than respiration (e.g., reaeration, weathering, and temperature changes) may also alter the value. Based on this, we acknowledge that the interpretations of the value in this study remain a working hypothesis that requires further studies to substantiate. For example, to better disentangle in situ production from externally sourced CO_2 contributions, future research should incorporate paired measurements of ecosystem metabolism and CO_2 to distinguish their roles in instream CO_2 dynamics from external sources. Such approaches would provide a more mechanistic understanding of how internal and external processes jointly regulate fluvial GHG dynamics across space and time.

5. Conclusions

This study revealed important insights into how agricultural intensification controls fluvial greenhouse gas (GHG) dynamics across contrasting climatic regions. We showed that fertilization intensity fundamentally alters the relative importance of stream size versus land use in controlling fluvial GHG fluxes. In tropical catchments with low-intensity agriculture, CO_2 and N_2O fluxes followed classical scaling patterns with stream size and discharge. However, in temperate catchments with high fertilization, nutrient enrichment became the dominant control, overriding the role of physical stream characteristics. We also found that the respiratory quotient (RQ) emerged as a promising proxy for identifying fluvial CO_2 sources across differing discharge periods. Specifically, we hypothesized that the variability in the RQ may distinguish between in-situ biogeochemical production and external inputs, with the dominance of these sources linked to upstream agricultural fertilization intensities. Taken together, these findings highlight that fertilization intensity may not only amplify GHG fluxes but also restructure their underlying controls and sources. This new understanding is critical as both agricultural intensification and extreme hydrological events are expected to intensify under future climate scenarios. Therefore, to ensure accurate fluvial GHG emissions reporting and effective mitigation policies, it is essential that models and mitigation strategies explicitly account for local-scale land use intensity and its distinct impact on fluvial GHG dynamics. This approach moves beyond one-size-fits-all solutions and tailors nutrient management to local agricultural contexts. For instance, promoting precision fertilization in both space and time, coupled with reducing nitrogen overuse in intensive agricultural regions, can substantially lower reactive nitrogen losses while enhancing yield efficiency and environmental sustainability. Furthermore, identifying regional emission hotspots through integrated monitoring and modeling frameworks enables the development of targeted mitigation strategies tailored to local soil–climate–management interactions. Building on the spatial variability revealed in this study, it is also crucial to refine IPCC emission factors and national greenhouse gas inventory methodologies, ensuring that global reporting systems more accurately capture spatial heterogeneity and region-specific management practices.

CRediT authorship contribution statement

Ricky Mwangada Mwanake: Writing – review & editing, Writing – original draft, Visualization, Formal analysis, Data curation, Conceptualization. **Gretchen Maria Gettel:** Writing – review & editing, Supervision, Conceptualization. **Elizabeth Gachibu Wangari:** Writing – review & editing, Data curation. **Klaus Butterbach-Bahl:** Writing – review & editing, Supervision, Conceptualization. **Ralf Kiese:** Writing – review & editing, Supervision, Funding acquisition, Conceptualization.

Funding

Infrastructure for the research was provided by the TERENO Bavarian Alps/Pre-Alps Observatory, funded by the Helmholtz Association through the joint program Changing Earth – Sustaining our Future (ATMO - PoF IV) program of Karlsruhe Institute of Technology (KIT), Germany. KBB received additional funding from the Danish National Research Foundation (DNRF), Grant Number P2 “Pioneer Center for Research in Sustainable Agricultural Futures (Land-CRAFT), Denmark.

Declaration of competing interest

The authors declare that they have no known competing financial interests or personal relationships that could have appeared to influence the work reported in this paper.

Acknowledgments

The authors would like to thank the entire laboratory staff at the ILRI Mazingira Lab, Kenya, Karlsruhe Institute of Technology, Campus Alpin, Justus Liebig University Giessen, and the University of Tübingen for helping to provide logistical support and for supporting the gas and nutrient analyses that yielded the source dataset.

Appendix A. Supplementary data

Supplementary data to this article can be found online at https://doi.org/10.1016/j.jenvman.2025.127782.

Data availability

My data links has been shared in the Manuscript

References

Aho, K.S., Fair, J.H., Hosen, J.D., Kyzivat, E.D., Logozzo, L.A., Rocher-Ros, G., Weber, L. C., Yoon, B., Raymond, P.A., 2021. Distinct concentration-discharge dynamics in temperate streams and rivers: CO2 exhibits chemostasis while CH4 exhibits source limitation due to temperature control. Limnol. Oceanogr. 66 (10), 3656–3668. https://doi.org/10.1002/lno.11906.

Aho, K.S., Fair, J.H., Hosen, J.D., Kyzivat, E.D., Logozzo, L.A., Weber, L.C., Yoon, B., Zarnetske, J.P., Raymond, P.A., 2022. An intense precipitation event causes a temperate forested drainage network to shift from N2O source to sink. Limnol. Oceanogr. 67 (S1), S242–S257. https://doi.org/10.1002/lno.12006.

Andrews, L.F., Wadnerkar, P.D., White, S.A., Chen, X., Correa, R.E., Jeffrey, L.C., Santos, I.R., 2021. Hydrological, geochemical and land use drivers of greenhouse gas dynamics in eleven sub-tropical streams. Aquat. Sci. 83 (2). https://doi.org/10.1007/s00027-021-00791-x.

Battin, T.J., Lauerwald, R., Bernhardt, E.S., Bertuzzo, E., Gener, L.G., Hall, R.O., Hotchkiss, E.R., Maavara, T., Pavelsky, T.M., Ran, L., Raymond, P., Rosentreter, J.A., Regnier, P., 2023. River ecosystem metabolism and carbon biogeochemistry in a changing world. Nature 613 (7944), 449–459. https://doi.org/10.1038/s41586-022-05500-8.

Baulch, H.M., Dillon, P.J., Maranger, R., Schiff, S.L., 2011. Diffusive and ebullitive transport of methane and nitrous oxide from streams: are bubble-mediated fluxes important? J. Geophys. Res.: Biogeosciences 116 (4). https://doi.org/10.1029/2011JG001656.

Bodmer, P., Heinz, M., Pusch, M., Singer, G., Premke, K., 2016. Carbon dynamics and their link to dissolved organic matter quality across contrasting stream ecosystems. Sci. Total Environ. 553, 574–586. https://doi.org/10.1016/j.scitotenv.2016.02.095.

Borges, A.V., Darchambeau, F., Lambert, T., Bouillon, S., Morana, C., Brouyère, S., Hakoun, V., Jurado, A., Tseng, H.C., Descy, J.P., Roland, F.A.E., 2018. Effects of agricultural land use on fluvial carbon dioxide, methane and nitrous oxide concentrations in a large European river, the Meuse (Belgium). Sci. Total Environ. 610–611, 342–355. https://doi.org/10.1016/j.scitotenv.2017.08.047.

Borges, A.V., Darchambeau, F., Teodoru, C.R., Marwick, T.R., Tamooh, F., Geeraert, N., Omengo, F.O., Guérin, F., Lambert, T., Morana, C., Okuku, E., Bouillon, S., 2015. Globally significant greenhouse-gas emissions from African inland waters. Nat. Geosci. 8 (8), 637–642. https://doi.org/10.1038/ngeo2486.

Dang, C., Kellner, E., Martin, G., Freedman, Z.B., Hubbart, J., Stephan, K., Kelly, C.N., Morrissey, E.M., 2021. Land use intensification destabilizes stream microbial biodiversity and decreases metabolic efficiency. Sci. Total Environ. 767, 145440. https://doi.org/10.1016/j.scitotenv.2021.145440.

DelVecchia, A.G., Rhea, S., Aho, K.S., Stanley, E.H., Hotchkiss, E.R., Carter, A., Bernhardt, E.S., 2023. Variability and drivers of CO2, CH4, and N2O concentrations in streams across the United States. Limnol. Oceanogr. 68 (2), 394–408. https://doi.org/10.1002/lno.12281.

Duvert, C., Hutley, L.B., Beringer, J., Bird, M.I., Birkel, C., Maher, D.T., Northwood, M., Rudge, M., Setterfield, S.A., Wynn, J.G., 2020. Net landscape carbon balance of a tropical savanna: relative importance of fire and aquatic export in offsetting terrestrial production. Glob. Change Biol. 26 (10), 5899–5913. https://doi.org/10.1111/gcb.15287.

Hall, R.O., Ulseth, A.J., 2020. Gas exchange in streams and rivers. WIREs Water 7 (1). https://doi.org/10.1002/wat2.1391.

Helton, A.M., Ardón, M., Bernhardt, E.S., 2015. Thermodynamic constraints on the utility of ecological stoichiometry for explaining global biogeochemical patterns. Ecol. Lett. 18 (10), 1049–1056. https://doi.org/10.1111/ele.12487.

Herreid, A.M., Wymore, A.S., Varner, R.K., Potter, J.D., McDowell, W.H., 2021. Divergent controls on stream greenhouse gas concentrations across a land-use gradient. Ecosystems 24 (6), 1299–1316. https://doi.org/10.1007/s10021-020-00584-7.

Ho, L., Jerves-Cobo, R., Barthel, M., Six, J., Bode, S., Boeckx, P., Goethals, P., 2022. Greenhouse gas dynamics in an urbanized river system: influence of water quality and land use. Environ. Sci. Pollut. Control Ser. 29 (25), 37277–37290. https://doi.org/10.1007/s11356-021-18081-2.

Hotchkiss, E.R., Hall, R.O., Sponseller, R.A., Butman, D., Klaminder, J., Laudon, H., Rosvall, M., Karlsson, J., 2015. Sources of and processes controlling CO2emissions change with the size of streams and rivers. Nat. Geosci. 8 (9), 696–699. https://doi.org/10.1038/ngeo2507.

Hynes, H.B.N., 1975. The stream and its valley. SIL Proceedings, 1922-2010 19 (1), 1–15. https://doi.org/10.1080/03680770.1974.11896033.

Jones, M.W., Peters, G.P., Gasser, T., Andrew, R.M., Schwingshackl, C., Gütschow, J., Houghton, R.A., Friedlingstein, P., Pongratz, J., Le Quéré, C., 2023. National contributions to climate change due to historical emissions of carbon dioxide, methane, and nitrous oxide since 1850. Sci. Data 10 (1). https://doi.org/10.1038/s41597-023-02041-1.

Kominoski, J.S., Rosemond, A.D., Benstead, J.P., Gulis, V., Manning, D.W.P., 2018. Experimental nitrogen and phosphorus additions increase rates of stream ecosystem respiration and carbon loss. Limnol. Oceanogr. 63 (1), 22–36. https://doi.org/10.1002/lno.10610.

Lauerwald, R., Allen, G.H., Deemer, B.R., Liu, S., Maavara, T., Raymond, P., Alcott, L., Bastviken, D., Hastie, A., Holgerson, M.A., Johnson, M.S., Lehner, B., Lin, P., Marzadri, A., Ran, L., Tian, H., Yang, X., Yao, Y., Regnier, P., 2023. Inland water greenhouse gas budgets for RECCAP2: 1. state-of-the-art of global scale assessments. Glob. Biogeochem. Cycles 37 (5). https://doi.org/10.1029/2022GB007657.

Li, M., Peng, C., Zhang, K., Xu, L., Wang, J., Yang, Y., Li, P., Liu, Z., He, N., 2021a. Headwater stream ecosystem: an important source of greenhouse gases to the atmosphere. Water Res. 190. https://doi.org/10.1016/j.watres.2020.116738.

Liu, B., Wang, Z., Tian, M., Yang, X., Chan, C.N., Chen, S., Yang, Q., Ran, L., 2023. Basin-scale CO_2 emissions from the East River in south China: importance of small Rivers, human impacts and monsoons. J. Geophys. Res.: Biogeosciences 128 (1).

Liu, S., Kuhn, C., Amatulli, G., Aho, K., Butman, D.E., Allen, G.H., Lin, P., Pan, M., Yamazaki, D., Brinkerhoff, C., Gleason, C., Xia, X., Raymond, P.A., 2022. The importance of hydrology in routing terrestrial carbon to the atmosphere via global streams and rivers. https://doi.org/10.1073/pnas.2106322119/-/DCSupplemental.

Marescaux, A., Thieu, V., Garnier, J., 2018. Carbon dioxide, methane and nitrous oxide emissions from the human-impacted Seine watershed in France. Sci. Total Environ. 643, 247–259. https://doi.org/10.1016/j.scitotenv.2018.06.151.

Marx, A., Dusek, J., Jankovec, J., Sanda, M., Vogel, T., van Geldern, R., Hartmann, J., Barth, J.A.C., 2017. A review of CO2 and associated carbon dynamics in headwater streams: a global perspective. Rev. Geophys. 55 (2), 560–585. https://doi.org/10.1002/2016RG000547.

Marzadri, A., Dee, M.M., Tonina, D., Bellin, A., Tank, J.L., 2017. Role of surface and subsurface processes in scaling N2O emissions along riverine networks. Proc. Natl. Acad. Sci. USA 114 (17), 4330–4335. https://doi.org/10.1073/pnas.1617454114.

Mwanake, R., 2023a. Water quality and greenhouse gas (GHG) concentration data for temperate headwater streams in Germany. In: Radar 4 KIT. Karlsruhe Institute of Technology (KIT); Karlsruhe Institute of Technology - Institute of Meteorology and Climate Research - Atmospheric Environmental Research (IMK-IFU). https://doi.org/10.35097/1684.

Mwanake, R., 2023b. Water quality and greenhouse gas (GHG) concentration data from streams and rivers in the tropical Mara basin. In: Radar 4 KIT. Karlsruhe Institute of Technology (KIT); Karlsruhe Institute of Technology - Institute of Meteorology and Climate Research - Atmospheric Environmental Research (IMK-IFU). https://doi.org/10.35097/1751.

Mwanake, R.M., Gettel, G.M., Aho, K.S., Namwaya, D.W., Masese, F.O., Butterbach-Bahl, K., Raymond, P.A., 2019. Land use, not stream order, controls N2O concentration and flux in the upper Mara River Basin, Kenya. J. Geophys. Res.: Biogeosciences 124 (11), 3491–3506. https://doi.org/10.1029/2019JG005063.

Mwanake, R.M., Gettel, G.M., Ishimwe, C., Wangari, E.G., Butterbach-Bahl, K., Kiese, R., 2022. Basin-scale estimates of greenhouse gas emissions from the Mara River, Kenya: importance of discharge, stream size, and land use/land cover. Limnol. Oceanogr. 67 (8), 1776–1793. https://doi.org/10.1002/lno.12166.

Mwanake, R.M., Gettel, G.M., Wangari, E.G., Butterbach-Bahl, K., Kiese, R., 2023b. Interactive effects of catchment mean water residence time and agricultural area on water physico-chemical variables and GHG saturations in headwater streams. Frontiers in Water 5. https://doi.org/10.3389/frwa.2023.1220544.

Mwanake, R.M., Gettel, G.M., Wangari, E.G., Glaser, C., Houska, T., Breuer, L., Butterbach-Bahl, K., Kiese, R., 2023a. Anthropogenic activities significantly increase annual greenhouse gas (GHG) fluxes from temperate headwater streams in Germany. Biogeosciences 20 (16), 3395–3422. https://doi.org/10.5194/bg-20-3395-2023.

Mwanake, R.M., Gettel, G.M., Wangari, E.G., Macharia, G.W., Martínez-Cuesta, R., Schulz, S., Schloter, M., Butterbach-Bahl, K., Kiese, R., 2025a. Elevated in-stream CO2 concentration stimulates net-N2O production from global fluvial ecosystems. Water Res. 287, 124320. https://doi.org/10.1016/j.watres.2025.124320.

Mwanake, R.M., Imhof, H.K., Kiese, R., 2024. Divergent drivers of the spatial variation in greenhouse gas concentrations and fluxes along the Rhine River and the Mittelland Canal in Germany. Environ. Sci. Pollut. Control Ser. https://doi.org/10.1007/s11356-024-33394-8.

Mwanake, R.M., Wangari, E.G., Winkler, K., Gretchen, G.M., Butterbach-Bahl, K., Kiese, R., 2025b. From data to insights: upscaling riverine GHG fluxes in Germany with machine learning. Sci. Total Environ. 958, 177984. https://doi.org/10.1016/j.scitotenv.2024.177984.

Park, J.-H., Lee, H., Zhumabieke, M., Kim, S.-H., Shin, K.-H., Khim, B.-K., 2023. Basin-specific pollution and impoundment effects on greenhouse gas distributions in three rivers and estuaries. Water Res. 236, 119982. https://doi.org/10.1016/j.watres.2023.119982.

Piatka, D.R., Nánási, R.L., Mwanake, R.M., Engelsberger, F., Willibald, G., Neidl, F., Kiese, R., 2024. Precipitation fuels dissolved greenhouse gas (CO2, CH4, N2O) dynamics in a peatland-dominated headwater stream: results from a continuous

monitoring setup. Frontiers in Water 5. https://doi.org/10.3389/frwa.2023.1321137.
Qin, X., Li, Y., Wan, Y., Fan, M., Liao, Y., Li, Y., Wang, B., Gao, Q., 2020. Diffusive flux of CH4 and N2O from agricultural river networks: regression tree and importance analysis. Sci. Total Environ. 717, 137244. https://doi.org/10.1016/j.scitotenv.2020.137244.
Quick, A.M., Reeder, W.J., Farrell, T.B., Tonina, D., Feris, K.P., Benner, S.G., 2019. Nitrous oxide from streams and rivers: a review of primary biogeochemical pathways and environmental variables. Earth Sci. Rev. 191, 224–262. https://doi.org/10.1016/j.earscirev.2019.02.021.
Raymond, P.A., Hartmann, J., Lauerwald, R., Sobek, S., McDonald, C., Hoover, M., Butman, D., Striegl, R., Mayorga, E., Humborg, C., Kortelainen, P., Dürr, H., Meybeck, M., Ciais, P., Guth, P., 2013. Global carbon dioxide emissions from inland waters. Nature 503 (7476), 355–359. https://doi.org/10.1038/nature12760.
Raymond, P.A., Zappa, C.J., Butman, D., Bott, T.L., Potter, J., Mulholland, P., Laursen, A. E., McDowell, W.H., Newbold, D., 2012. Scaling the gas transfer velocity and hydraulic geometry in streams and small rivers. Limnol. Oceanogr. Fluid. Environ. 2 (1), 41–53. https://doi.org/10.1215/21573689-1597669.
Richey, J.E., Devol, A.H., Wofsy, S.C., Victoria, R., Riberio, M.N.G., 1988. Biogenic gases and the oxidation and reduction of carbon in amazon River and floodplain waters. Limnol. Oceanogr. 33 (4), 551–561. https://doi.org/10.4319/lo.1988.33.4.0551.
Rocher-Ros, G., Stanley, E.H., Loken, L.C., Casson, N.J., Raymond, P.A., Liu, S., Amatulli, G., Sponseller, R.A., 2023. Global methane emissions from rivers and streams. Nature. https://doi.org/10.1038/s41586-023-06344-6.
Schade, J.D., Bailio, J., McDowell, W.H., 2016. Greenhouse gas flux from headwater streams in New Hampshire, USA: patterns and drivers. Limnol. Oceanogr. 61, S165–S174. https://doi.org/10.1002/lno.10337.
Stanley, E.H., Casson, N.J., Christel, S.T., Crawford, J.T., Loken, L.C., Oliver, S.K., 2016. The ecology of methane in streams and rivers: patterns, controls, and global significance. Ecol. Monogr. 86 (2), 146–171. https://doi.org/10.1890/15-1027.
Taylor, P.G., Townsend, A.R., 2010. Stoichiometric control of organic carbon-nitrate relationships from soils to the sea. Nature 464 (7292), 1178–1181. https://doi.org/10.1038/nature08985.
Upadhyay, P., Prajapati, S.K., Kumar, A., 2023. Impacts of riverine pollution on greenhouse gas emissions: a comprehensive review. Ecol. Indic. 154, 110649. https://doi.org/10.1016/j.ecolind.2023.110649.
Václavík, T., Lautenbach, S., Kuemmerle, T., Seppelt, R., 2013. Mapping global land system archetypes. Glob. Environ. Change 23 (6), 1637–1647. https://doi.org/10.1016/j.gloenvcha.2013.09.004.
Wachholz, A., Dehaspe, J., Ebeling, P., Kumar, R., Musolff, A., Saavedra, F., Winter, C., Yang, S., Graeber, D., 2023. Stoichiometry on the edge—humans induce strong imbalances of reactive C:N:P ratios in streams. Environ. Res. Lett. 18 (4). https://doi.org/10.1088/1748-9326/acc3b1.
Wallin, M.B., Campeau, A., Audet, J., Bastviken, D., Bishop, K., Kokic, J., Laudon, H., Lundin, E., Löfgren, S., Natchimuthu, S., Sobek, S., Teutschbein, C., Weyhenmeyer, G.A., Grabs, T., 2018. Carbon dioxide and methane emissions of Swedish low-order streams—a national estimate and lessons learnt from more than a decade of observations. Limnology And Oceanography Letters 3 (3), 156–167. https://doi.org/10.1002/lol2.10061.
Wan, L., Kendall, A.D., Martin, S.L., Hamlin, Q.F., Hyndman, D.W., 2023. Important role of overland flows and tile field pathways in nutrient transport. Environ. Sci. Technol. 57 (44), 17061–17075. https://doi.org/10.1021/acs.est.3c03741.
Wang, S., Lan, B., Yu, L., Xiao, M., Jiang, L., Qin, Y., Jin, Y., Zhou, Y., Armanbek, G., Ma, J., Wang, M., Jetten, M.S.M., Tian, H., Zhu, G., Zhu, Y.G., 2024. Ammonium-derived nitrous oxide is a global source in streams. Nat. Commun. 15 (1). https://doi.org/10.1038/s41467-024-48343-9.
Woodrow, R.L., White, S.A., Conrad, S.R., Wadnerkar, P.D., Rocher-Ros, G., Sanders, C. J., Holloway, C.J., Santos, I.R., 2024. Enhanced stream greenhouse gas emissions at night and during flood events. Limnology and Oceanography Letters 9 (3), 276–285. https://doi.org/10.1002/lol2.10374.
Yao, Y., Tian, H., Shi, H., Pan, S., Xu, R., Pan, N., Canadell, J.G., 2020. Increased global nitrous oxide emissions from streams and rivers in the Anthropocene. Nat. Clim. Change 10 (2), 138–142. https://doi.org/10.1038/s41558-019-0665-8.
Zannella, A., Eklöf, K., Lannergård, E., Laudon, H., Maher Hasselquist, E., Wallin, M.B., 2023. Metabolic processes control carbon dioxide dynamics in a boreal forest ditch affected by clear-cut forestry. Frontiers in Water 5. https://doi.org/10.3389/frwa.2023.1250068.
Zou, H., Hastie, T., 2005. Regularization and variable selection via the elastic net. J. Roy. Stat. Soc. B Stat. Methodol. 67 (2), 301–320. https://doi.org/10.1111/j.1467-9868.2005.00503.x.